Cancer Chemotherapy and Pharmacology
https://doi.org/10.1007/s00280-020-04033-z

ORIGINAL ARTICLE

Novel complementary antitumour effects of celastrol and metformin by targeting IκBκB, apoptosis and NLRP3 inflammasome activation in diethylnitrosamine-induced murine hepatocarcinogenesis

Sameh Saber[1] · Amal M. H. Ghanim[2] · Eman El-Ahwany[3] · Eman M. Abd El-Kader[1]

Received: 27 September 2019 / Accepted: 13 January 2020

Abstract

One promising strategy for minimizing chemotherapeutic resistance in hepatocellular carcinoma (HCC) is the use of effective chemosensitizers. We studied the complementary multi-targeted molecular mechanisms of metformin and celastrol in mice with diethylnitrosamine-induced HCC to investigate whether metformin could augment the sensitivity of HCC tissue to the effect of celastrol. Simultaneous administration of celastrol (2 mg/kg) and metformin (200 mg/kg) improved liver function, enhanced the histological picture and prolonged survival. Additionally, combination therapy exerted anti-inflammatory activity, as indicated by the decreased levels of TNF-α and IL-6. This protective role could be attributed to inhibition of inflammasome activation. Herein, our data revealed downregulated NLRP3 gene expression, suppressed caspase-1 activity and reduced levels of the active forms of IL-1β and IL-18. Under this condition, pyroptotic activity was suppressed. In contrast, in the celastrol and celastrol + metformin groups, the apoptotic potential was amplified, as revealed by the increase in the caspase-9 and caspase-3 levels and Bax:BCL-2 ratio. In addition to their repressive effect on the gene expression of NFκBp65, TNFR and TLR4, metformin and celastrol inhibited phosphorylation-induced activation of IκBκB and NFκBp65 and decreased IκBα degradation. Combination therapy with metformin and celastrol repressed markers of angiogenesis, metastasis and tumour proliferation, as revealed by the decreased hepatic levels of VEGF, MMP-2/9 and cyclin D1 mRNA, respectively. In conclusion, by inhibiting NLRP3 inflammasome and its prerequisite NFκB signalling, simultaneous administration of metformin and celastrol appears to have additive benefits in the treatment of HCC compared to cela monotherapy. This effect warrants further clinical investigation.

Keywords HCC/diethylnitrosamine · NLRP3 inflammasome · Metformin/celastrol · Iκbκb · Caspase-1 · Apoptosis · NFκBp65 · Bax/BCL-2 · TLR4 · IκBα

Abbreviations

AFP	Alpha-fetoprotein
AKT	Protein kinase B
Bax	BCL-2 associated × protein
BCL-2	B-cell lymphoma-2
cel	Celastrol
ECM	Extracellular matrix
DEN	Diethylnitrosamine
GAPDH	Glyceraldehyde 3-phosphate dehydrogenase
HCC	Hepatocellular carcinoma
IκBα	IκBκB: the inhibitor κB kinase complex
MAPK	Mitogen-activated protein kinase
MDA	Malondialdehyde
met	Metformin
MMP	Matrix metalloproteinase
NFκB	Nuclear transcription factor kappa B
NLRP3	Nod-like receptor protein 3

Electronic supplementary material The online version of this article (https://doi.org/10.1007/s00280-020-04033-z) contains supplementary material, which is available to authorized users.

✉ Sameh Saber
Sameh.mohamed@deltauniv.edu.eg;
sampharm81@gmail.com

[1] Department of Pharmacology, Faculty of Pharmacy, Delta University for Science and Technology, International Coastal Road, Gamasa City, P.O. Box: +11152, Mansoura, Dakahlia, Egypt

[2] Department of Biochemistry, Faculty of Pharmacy, Delta University for Science and Technology, Gamasa City, Mansoura, Egypt

[3] Department of Immunology, Theodor Bilharz Research Institute, Giza, Egypt

Published online: 27 January 2020

PI3K	Phosphoinositide 3-kinase
TLR	Toll like receptor
TNF-α	Tumour necrosis factor-alpha
VEGF	Vascular endothelial growth factor

Introduction

Hepatocellular carcinoma (HCC) is the most common form of liver malignancy and is considered a leading cause of cancer-related mortality worldwide. HCC is commonly associated with high incidence, high recurrence and relapse rates, poor prognosis, and high chemotherapeutic resistance potential. In addition, current systemic therapies such as sorafenib have been shown to affect patients' survival by only a few months [1]. These facts have led many researchers to explore the underlying mechanisms by which liver cancer cells develop and proliferate in an attempt to improve the efficiency of strategies for HCC management.

There are no currently NLRP3 antagonists approved for therapeutic purposes. Inflammasomes are cytoplasmic multiprotein signalling complexes that are produced as an inflammatory immune response to diverse signals. Dysregulation of Nod-like receptor protein 3 (NLRP3) inflammasome activation is extensively linked with various malignancies. The role of the NLRP3 inflammasome in livers with HCC has been confirmed by evidence. Pharmacological intervention with NLRP3 inflammasome activation may suppress proliferation, invasion and metastasis in HCC, suggesting a potential therapeutic strategy [2]. Toll-like receptor (TLR)/nuclear transcription factor kappa B (NFκB) pathway activation mediates the transcriptional upregulation and oligomerization of NLRP3 components and the subsequent activation of caspase-1 which, in turn, mediates the proinflammatory cell death process of pyroptosis and increases the secretion of inflammasome effector molecules, for example, the proinflammatory cytokines IL-1β and IL-18 [3].

NFκB proteins, the key regulators of innate and adaptive immune responses, are induced in many types of cancers, including HCC and are strongly related to tumour proliferation, invasion and metastasis as well as apoptosis inhibition [4]. Activation of the NFκB signalling pathway begins with site-specific phosphorylation of the inhibitor of kappa B alpha (IκBα) by the inhibitor κB kinase complex (IκBκB), followed by IκBα ubiquitination and degradation by the proteasome, leading to NFκB nuclear translocation [5]. The NFκB signalling pathway modulates the transcription of several genes associated with cancer cell apoptosis (BCL-2 family proteins), as well as tumour proliferation (Cyclin D1) and metastasis (MMP-2 and -9). In addition, this pathway plays a significant role in the transcription of genes encoding several proinflammatory regulators, such as TNF-α, IL-1β and IL-6 [6]. Therefore, several studies have explored the inhibitory effect of numerous anticancer drugs on NFκB signalling by targeting many steps in the NFκB activation pathway.

Many studies have revealed the anticancer and anti-inflammatory activity of the bioactive triterpene celastrol (cela), isolated from *Tripterygium wilfordii* root bark. The cytotoxic activity of cela against tumours has been attributed to its modulation of diverse molecular pathways, particularly its suppression of the NFκB signalling pathway and its target genes. Cela inhibits NFκB activation by stabilizing the IκB/NFκB complex, preventing IκBα protein degradation and NFκB nuclear translocation. This effect results in downregulated transcription of several NFκB target genes [7]. Despite the therapeutic potential of cela as an anticancer agent, its further clinical application is still limited by its associated adverse reactions. Data from rodents demonstrated an LD_{50} of 20.5 mg/kg. In addition, other reports revealed that a dose of 4 mg/kg was associated with a mortality rate of 40% [8].

Metformin (met) is mainly used as a synthetic hypoglycaemic drug; however, many studies have reported that met elicited noticeable anti-inflammatory activity. This anti-inflammatory effect has been attributed to inhibition of NFκB signalling [9]. In addition, many reports have shed light on the anticancer potential of met [10]. Some studies proposed that the reduction in chronic inflammatory responses and TNF-α production, as well as the inhibition of NFκB activation by met, could help inhibit tumour development, promote tumour cell apoptosis and inhibit cancer cell proliferation and metastasis [11]. However, the molecular mechanisms underlying the anticancer activity of met need further clarification, particularly in the management of HCC.

One promising strategy for minimizing chemotherapeutic resistance is the use of effective chemosensitizers. After an extensive literature review, the low cost and low toxicity, in addition to the complementary multi-targeted antitumour molecular mechanisms, prompted us to suggest that met could sensitize HCC model livers to the effect of cela. The expected chemosensitizing properties of met could be mediated through its ability to modulate multiple cell signalling molecules, including NFκB and inflammasome activation.

There are no currently NLRP3 antagonists approved for therapeutic purposes. Therefore, in the current study, we aimed to investigate whether met could be an ideal candidate adjunct to cela in the treatment of diethylnitrosamine-induced HCC in mice. Combined therapy with met and cela was expected to exhibit synergistic antitumour activity, suggesting a promising treatment option combating resistance, minimizing toxicity and cost, and enhancing survival.

Materials and methods

Animals

Male BALB/c mice, weighing 25 ± 2 g and age 6–8 weeks, were purchased from the animal facility at Delta University for Science and Technology. They were maintained under pathogen-free conditions in polypropylene cages and allowed free access to rodent chow (23% protein and 4% fat) and water ad libitum. They were let for a 1 week of acclimatization before initiating the experiment. Standard laboratory conditions (21 °C, 45–55% humidity) and light/dark cycles (12:12 h) were maintained. All animal experiments complied with the guidelines of the Institutional Animal Care and Use Committee of the Faculty of Pharmacy at Delta University for Science and Technology (approval number: FPDU2019/119) and followed the standards equivalent to the UKCCCR guidelines for the welfare of animals in experimental neoplasia Br J Cancer 58: 109–113, [12]. In addition, experimental protocols comply with the ARRIVE guidelines [13] and carried out in accordance with the U.K. Animals (Scientific Procedures) Act, 1986 and associated guidelines, EU Directive 2010/63/EU for animal experiments [14].

Experimental design

Mice were randomly allocated to seven groups of 20 mice each. Mice in the Normal group received weekly i.p. injections of normal saline solution (NSS) for 10 weeks. Mice in the Normal/met group received weekly i.p. injections of NSS for 10 weeks, followed by met (200 mg/kg/day, p.o.). Mice in the Normal/cela group received weekly i.p. injections of NSS for 10 weeks, followed by cela (2 mg/kg/day, p.o.). Mice in the DEN group received weekly i.p. injections of 100 mg/kg 1% diethylnitrosamine (DEN) (v/v) in NSS for 10 weeks. Mice in the DEN/met group received weekly i.p. injections of 100 mg/kg 1% DEN (v/v) in NSS for 10 weeks, followed by met (200 mg/kg/day, p.o.). Mice in the DEN/cela group received weekly i.p. injections of 100 mg/kg 1% DEN (v/v) in NSS for 10 weeks, followed by cela (2 mg/kg/day, p.o.) afterwards. Mice in the DEN/met + cela group received weekly i.p. injections of 100 mg/kg 1% DEN (v/v) in NSS for 10 weeks, followed by met (200 mg/kg/day, p.o.) + cela (2 mg/kg/day, p.o.). Drug treatment started on day 75 and continued to the end of the experiment, up to day 150 (Table 1).

Calculation of relative liver weight

The relative liver weight was calculated as the liver weight (g) divided by the body weight (g).

Liver tumour examination

After careful removal and washing of livers in chilled PBS, the number of surface nodules (≥ 1 mm diameter) of all lobes were counted. Non-tumourous tissue from the largest lobe of each animal was harvested for RNA and protein extraction for further biochemical measurements. Histologic sections including tumourous tissues were separated and fixed in 4% neutral buffered formalin for 24 h prior to histological examination.

Histopathological examination

Liver tissues were fixed in paraffin. Paraffin–beeswax tissue blocks were sectioned at a 4-µm thickness with a sledge microtome. Tissue sections were collected on glass slides, deparaffinized, stained with haematoxylin and eosin (H&E) and examined with an electric light microscope [15].

Table 1 Experimental design

Exp. groups	Days (1:75)	Days (75:150)
Normal group	i.p. injections of NSS once a week	–
Normal/met group	i.p. injections of NSS once a week	met 200 mg/kg/p.o./day
Normal/cela group	i.p. injections of NSS once a week	cela 2 mg/kg/p.o./day
DEN group	i.p. injections of 100 mg/kg of 1% DEN (v/v) in NSS once a week	–
DEN/met group	i.p. injections of 100 mg/kg of 1% DEN (v/v) in NSS once a week	met 200 mg/kg/p.o./day
DEN/cela group	i.p. injections of 100 mg/kg of 1% DEN (v/v) in NSS once a week	cela 2 mg/kg/p.o./day
DEN/met + cela	i.p. injections of 100 mg/kg of 1% DEN (v/v) in NSS once a week	met 200 mg/kg/p.o./day + cela 2 mg/kg/p.o./day

cela celastrol, *DEN* diethylnitrosamine, *i.p.* intraperitoneal, *met* metformin, *NSS* normal saline solution, *p.o.* per oral

Biochemical analysis

Assessment of AFP and MDA

Following the manufacturer's protocol, ELISA kits supplied from R&D systems (Minneapolis, MN, USA) were used for the determination of mouse AFP. MDA is a marker for oxidative stress that condenses with two equivalents of thiobarbituric acid to give a fluorescent red derivative that can be assayed using commercially available kits from Biodiagnostic Co. (Giza, Egypt).

Assessment of ALT, AST, ALP, and γGT

ALT, AST, ALP, and γGT were measured spectrophotometrically using commercially available kits from Bio-diagnostic Co. in accordance with the manufacturer's instructions.

Assessment of hepatic levels of IL-1β, IL-18, TNF-α, and IL-6

For the determination of IL-1β, ELISA kits purchased from BioLegend (San Diego, CA, USA) were used as per the manufacturer's instructions. IL-18 hepatic levels were measured using ELISA kits supplied by USCN Life Science Inc. (Wuhan, China) as instructed. In accordance with the given protocol, mouse quantikine ELISA kits purchased from R&D systems were used for the determination of TNF-α and IL-6.

Assessment of VEGF, MMP-2 and MMP-9

MMP-2 and MMP-9 hepatic levels were measured using ELISA kits supplied by CUSABIO (Wuhan, China). VEGF was measured in the liver by ELISA kit purchased from R&D systems according to the manufacturer's instructions.

Assessment of caspase-1 activity

Determination of caspase-1 activity was based on spectrophotometric detection of the chromophore p-nitroanilide (p-NA) after cleavage from the labelled substrate YVAD-p-NA using a caspase-1 colorimetric assay kit from R&D Systems. p-NA light emission at 405 nm was quantified using a microtiter plate reader. Briefly, tissue lysates were prepared using chilled lysis buffer and were centrifuged at 10,000×*g*. The protein concentration of the cytosolic extracts was assayed. One hundred micrograms of protein was diluted in 50 µl of lysis buffer. Fifty microlitres of 2× reaction buffer (containing 10 mM DTT) and 5 µl of YVAD-p-NA substrate was added to each sample and incubated at 37 °C for 1–2 h. Samples were read at 405 nm in a microtitre plate reader. The results are expressed as the fold increase in caspase-1 activity relative to the Normal group.

Assessment of hepatic caspase-3, caspase-9, BCL-2 and Bax levels

After preparation of tissue lysates, protein quantification was performed with a BCA protein assay reagent kit obtained from Thermo Fisher Scientific Inc. (Rockford, USA). Cleaved caspase-3 (Asp175) levels were measured with a mouse DuoSet IC ELISA kit from R&D systems. The levels were normalized to the total protein concentrations. Hepatic caspase-9 levels were assessed using ELISA kits supplied by MyBioSource Inc. (San Diego, CA, USA). BCL-2 levels were measured using a kit from Abbexa (Cambridge, UK). Bax levels were measured using a kit obtained from MyBioSource Inc., in accordance with the manufacturer's instructions.

Assessment of IκBα and NFκB p65 (pSer536) levels

IκBα levels were measured with an ELISA kit obtained from CUSABIO, according to the manufacturer's instructions. NFκB P65 (pSer536) was measured with an ELISA kit purchased from Abcam (Cambridge, MA, USA). Briefly, 10 ml of 1× cell extraction buffer PTR was prepared by combining 7.8 ml of deionized water, 2 ml of 5× cell extraction buffer PTR and 200 µl of 50× cell extraction enhancer solution. One millilitre of 1× cell extraction buffer PTR was used to homogenize liver tissue by incubation on ice for 20 min and centrifugation at 18,000×*g* for 20 min at 4 °C. Pellets were discarded and supernatants were transferred to clean tubes in preparation for protein quantification. Then, 1× cell extraction buffer PTR was used to dilute samples to the desired volume. Samples were subjected to the SimpleStep ELISA protocol following the manufacturer's instructions. Finally, the levels were normalized to the level of NFκB P65 (total) protein measured in the same sample.

Assessment of IκBκB

Harvested livers were rinsed with PBS, ground in ice-cold buffer into 1–2 mm pieces and homogenized using an extraction buffer containing 100 mM Tris (pH 7.4), 150 mM NaCl, 1 mM EGTA, 1 mM EDTA, 1% Triton X-100, and 0.5% sodium deoxycholate. Immediately before use, 1 mM phenylmethylsulfonyl fluoride (PMSF), phosphatase inhibitor cocktail and protease inhibitor cocktail were added. Samples were placed on a shaker at 4 °C for 1 h and were then centrifuged at 10,000×*g* for 5 min. Total protein concentration was measured with BCA reagent to normalize the volume of each sample. A PathScan (Cell Signaling Technology, Danvers, MA, USA) sandwich ELISA kit was used to measure the endogenous levels of IκBκB (pSer177/181) and total GAPDH in accordance with the manufacturer's protocol. The optical density (OD) values of IκBκB (pSer177/181)

were normalized to the total GAPDH level measured in the same sample.

Quantitative real-time PCR (qPCR) analysis of NFκB p65, cyclin D1, IκBα, TNFR, TLR4, and NLRP3 expression

An RNeasy Mini Kit (Qiagen, Germany) was used to extract total RNA from liver tissues in an RNase-free environment, according to the manufacturer's instructions. A NanoDrop 2000 spectrophotometer (Thermo Scientific, USA) was used to measure the RNA concentration and purity. RNA (2 µg) was reverse transcribed with Quantiscript reverse transcriptase (QuantiTect Reverse Transcription Kit, Qiagen, Germany). A Rotor-Gene Q thermocycler (Qiagen, Hilden, Germany) and SYBR Green PCR Master Mix (Qiagen, USA) were used to perform PCR. qPCR was performed in triplicate and included no-template controls. The sequences of the PCR primer pairs are shown in Online Resource 1. The relative expression values of the studied genes were calculated using the comparative cycle threshold (Ct) ($2^{-\Delta\Delta CT}$) method. All values were normalized to the expression of the β-actin gene as the invariant endogenous control in the same sample. Rotor-Gene Q Software 2.1 (Qiagen) was used for data analysis.

Statistical analysis

Statistical analyses were performed using GraphPad Prism software (GraphPad Software Inc. V6.01, San Diego, CA, USA). One-way analysis of variance (ANOVA) followed by the Tukey–Kramer post hoc test for multiple comparisons was used to assess significant differences between groups for parametric data, the Kruskal–Wallis test followed by Dunn's post hoc test was used for non-parametric data (examination of liver surface nodules), and linear regression analysis for the best-fit line was used to construct the standard curves. For mortality assessment, the log-rank (Mantel–Cox) test was carried out to determine the significance of between-group differences in the Kaplan–Meier survival analysis. Data are expressed as the means ± standard deviations (SDs). Statistical significance was set at $p < 0.05$.

Results

Effect on relative liver weights

Significant increases in the liver weight:body weight ratios are commonly observed in conjunction with different types of neoplasia, including HCC. We observed a significant increase in the relative liver weights in DEN-treated mice compared with Normal group mice, which was attributed to the development of HCC nodules. Drug treatment, particularly combination therapy, significantly diminished the DEN-induced increase in the relative liver weights, indicating inhibition of neoplastic progression (Online Resource 2).

Effect on liver surface nodules

Grossly, with the naked eye, HCC nodules were apparent on the external surface and indicated high tumour development rates (Online Resource 3). We observed a significant increase in the number of surface nodules in the livers of DEN-treated mice compared with Normal group mice. However, the number of these nodules was significantly decreased in the treatment groups compared to the DEN-treated group. In addition, the number of surface nodules was significantly decreased after combination therapy compared with met or cela monotherapy (Online Resource9, panel a).

Histopathological examination

Tissue sections from Normal group mice showed a normal histological structure of the central vein and surrounding hepatocytes and no histological alterations (Online Resource 4, panel a). Similarly, no histopathological alterations were found in the tissues from the Normal/met (Online Resource 4, panel b) and Normal/cela groups (Online Resource 4, panel c). Liver sections from untreated mice with DEN-induced HCC exhibited multiple circumscribed foci of anaplastic hepatocytes that were well demarcated from their surroundings. The trabecular pattern of HCC (Online Resource 5, panel a, b), anaplastic cells with mitotic activity (Online Resource 5, panel c, arrow), karyomegaly and pleomorphism (Online Resource 5, panel c, arrowhead), hyperchromasia (Online Resource 5, panel d, arrow), and binucleated giant hepatocytes (Online Resource 5, panel d, arrowhead) were also seen. In addition, fatty changes and oval cell proliferation were seen in the adjacent parenchyma (Online Resource 5, panel e, f; arrowhead). Moreover, multiple focal, circumscribed, round eosinophilic bodies were noted to replace some hepatocytes (Mallory bodies) (Online Resource 5, panel g, h; arrow).

On the other hand, sections from the livers of mice with DEN-induced HCC and treated with met showed a wide focal area of degenerative changes in the parenchyma, which most likely developed as a result of HCC tumour growth inhibition and regression of malignancy (Online Resource 6, panel a, b). Additionally, Online Resource 6, panel c shows different degenerative changes in most hepatocytes throughout the parenchyma associated with inflammatory cell infiltration between cells. Further, massive inflammatory cell infiltration limited to the portal area (Online Resource 6, panel d, arrowhead) and associated with dilatation of the

portal vein (Online Resource 6, panel d, arrow) was seen. Tissue sections from the livers of mice with DEN-induced HCC and treated with cela showed regression of malignant changes associated with marked apoptosis and inflammatory cell infiltration between hepatocytes, limited to the area surrounding the dilated central vein (Online Resource 7, panel a, b; arrows). The portal area showed dilatation of the portal vein (Online Resource 7, panel c) and inflammatory cell infiltration limited to the area surrounding the bile ducts (Online Resource 7, panel d, arrow). Specimens from the livers of mice with DEN-induced HCC and treated with simultaneous administration of met and cela exhibited a marked appearance of apoptotic cells (Online Resource 8, panel a, b; arrows). The portal area showed minimal inflammatory cell infiltration surrounding the bile ducts and minimal dilatation of the portal vein (Online Resource 8, panel c, arrow).

Effect on the serum alpha-fetoprotein (AFP) level and hepatic malondialdehyde (MDA) content

Elevated levels of AFP are associated with active HCC. Coincident with the macroscopic evaluation of tumour nodules, the level of AFP was significantly elevated in the DEN-treated group compared to the Normal group and significantly decreased after drug treatment, particularly in the DEN/met + cela group, compared to the Normal group (Online Resource 9, panel b). Similarly, the hepatic level of MDA, the lipid peroxidation marker, was significantly higher in the DEN-treated group than in the Normal group and was significantly decreased after drug treatment, particularly in the DEN/met + cela group, compared to the Normal group, indicating an improved antioxidant status of the liver tissue (Online Resource 9, panel c).

Effect on alanine aminotransferase (ALT), aspartate aminotransferase (AST), alkaline phosphatase (ALP), and gamma-glutamyltransferase (γGT) levels

Elevated liver enzymes are an indication of liver inflammation and hepatocyte injury. Generally, the levels of liver enzymes are usually abnormal during the course of experimentally induced hepatocarcinogenesis. However, our results revealed that met, cela and, particularly, the combination significantly repressed the DEN-induced increase in liver function enzymes (Online Resource 10, panel a, b, c, d).

Effect on caspase-1 activity and IL-1β and IL-18 levels

The inflammasome is a multi-protein intracellular complex that mediates pyroptosis through the activation of caspase-1. Caspase-1 is essential for proteolytic cleavage of the pro-forms of IL-1β and IL-18 into the corresponding active cytokines. We found significant repression of caspase-1 activity after treatment with met or cela compared to that in DEN-treated mice and found that this inhibitory effect was amplified with combination therapy compared to either monotherapy (Online Resource 11, panel a).

IL-1β is a proinflammatory cytokine that is synthesized in response to inflammatory stimuli as an inactive pro-form that accumulates in the cytosol. Cleavage of pro-IL-1β into the active protein requires inflammasome activation. Moreover, elevated levels of IL-1β have been associated with many inflammatory conditions. Herein, we found a significant increase in the level of IL-1β in DEN-treated mice compared to Normal group mice, and noted a significant reduction in the IL-1β level after drug treatment, particularly combination therapy (Online Resource 11, panel b). Inflammasome activation results in IL-18 processing and secretion. We observed that drug treatment, including combination therapy, suppressed the DEN-induced increase in the level of IL-18, indicating a low level of inflammasome activation (Online Resource 11, panel c).

Effect on the gene expression of NLRP3

Nlrp3 is a component of the inflammasome. Dysregulation of NLRP3 inflammasome activation is involved in tumour pathogenesis. The significant increase in the level of NLRP3 mRNA expression in DEN-treated mice compared to Normal mice confirmed its implication in the pathogenesis of HCC. Both cela monotherapy and combination therapy significantly curbed NLRP3 gene expression with respect to that in the DEN-treated group. On the other hand, met monotherapy exhibited a strong trend towards a significant difference ($p = 0.09$) compared to DEN treatment (Fig. 1).

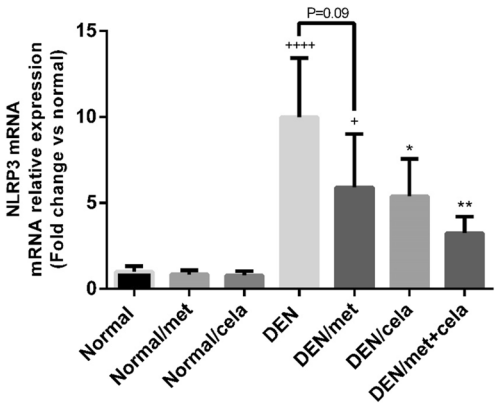

Fig. 1 Effects of met (200 mg/kg), cela (2 mg/kg) and combination therapy on the relative expression level of NLRP3 mRNA in the DEN-induced HCC mouse model. The data are presented as the means ± SDs. $+P < 0.05$ vs. Normal, $++++P < 0.0001$ vs. Normal. $*P < 0.05$ vs. DEN $**P < 0.01$ vs. DEN

Effect on the Bax:BCL-2 ratio and the levels of caspase-9 and caspase-3

The Bax:BCL-2 ratio is a marker of the apoptotic potential. In the current study, compared with the DEN-treated group, the groups treated with cela and the combination therapy exhibited a significant increase in the Bax:BCL-2 ratio (Fig. 2a). Caspase-9 and caspase-3 command a major defence strategy that prevents cells from acquiring carcinogenic potential. Our results revealed that cela and combination therapy with met + cela significantly overcame the DEN-induced decline in the levels of caspase-9 (Fig. 2b) and caspase-3 (Fig. 2c), with the most pronounced effect in the combination therapy group. These results revealed that met did not successfully induce a significant change in the apoptotic potential of HCC cells in the liver. However, met successfully augmented sensitivity of liver tissues to the effect of cela.

Effect on the gene expression levels of IκBα and NFκB p65

IκBα inhibits NFκB by preventing its nuclear translocation and keeping it sequestered in an inactive state in the cytosol; moreover, it inhibits the DNA binding ability of the NFκB transcription factor, a prerequisite for its transcriptional activity. In the present work, met + cela-treated mice exhibited a significant reduction in IκBα gene expression compared to DEN-treated mice. In this context, the gene expression of IκBα was inhibited due to the stabilization of its protein level. However, as a monotherapeutic agent, cela showed an increased tendency to significantly change this level ($p = 0.07$). This result revealed the chemosensitization potential of met treatment, although the change was non-significant compared to that with cela (Fig. 3a). On the other hand, mice in all treatment groups displayed a significant reduction in NFκB p65 gene expression compared with DEN-treated

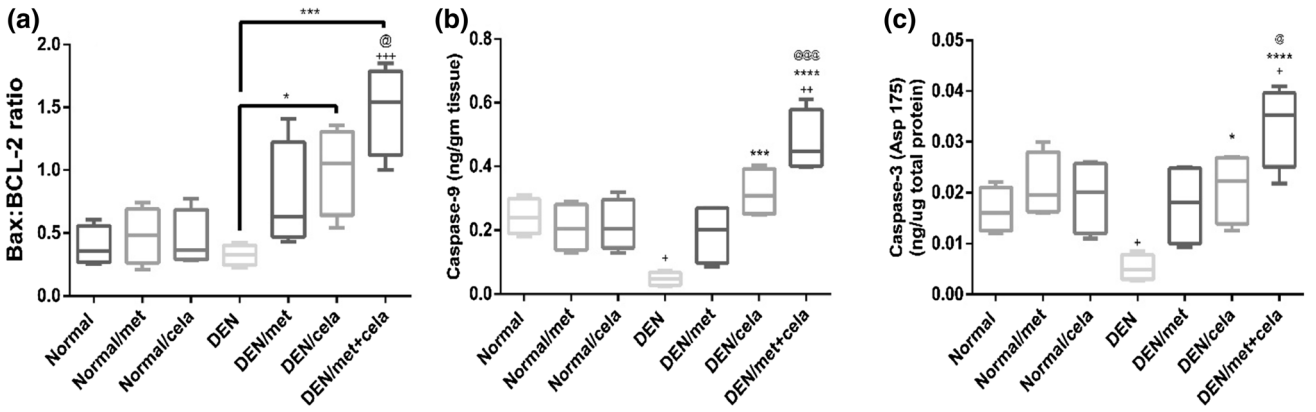

Fig. 2 Effects of met (200 mg/kg), cela (2 mg/kg) and combination therapy on **a** the Bax:BCL-2 ratio, **b** the hepatic level of caspase-9, and **c** the hepatic level of caspase-3 (pAsp175) in the DEN-induced HCC mouse model. The data are presented as the means ± SDs. $+P<0.05$ vs. Normal, $++P<0.01$ vs. Normal, $+++P<0.001$ vs. Normal. $*P<0.05$ vs. DEN, $***P<0.001$ vs. DEN, $****P<0.0001$ vs. DEN. $@P<0.05$ vs. DEN + met, $@@@P<0.001$ vs. DEN + met

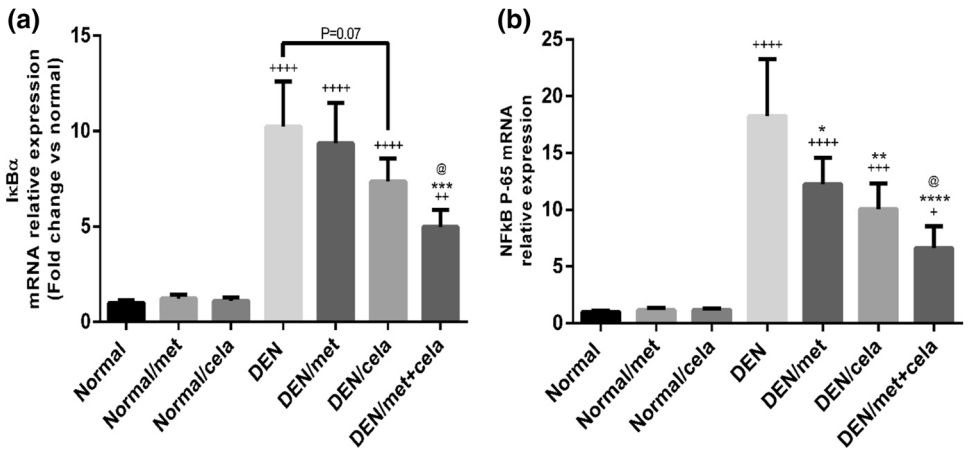

Fig. 3 Effects of met (200 mg/kg), cela (2 mg/kg) and combination therapy on the mRNA relative expression of **a** IκBα, and **b** NFκB P65 in DEN-induced HCC mouse model. The data are presented as the mean ± SD. $+P<0.05$ vs. Normal, $++P<0.01$ vs. Normal, $+++P<0.001$ vs. Normal, $++++P<0.0001$ vs. Normal; $*P<0.05$ vs. DEN, $**P<0.01$ vs. DEN, $***P<0.001$ vs. DEN, $****P<0.0001$ vs. DEN; $@P<0.05$ vs. DEN + met

mice, with the most pronounced effect in met + cela-treated mice (Fig. 3b).

Effect on the levels of IκBκB (pSer177/181), IκBα and NFκB p65 (pSer536)

Compared to DEN treatment only, met treatment exhibited a high tendency to significantly reduce ($p = 0.085$) the level of IκBκB (pSer177/181), while cela-treated and, particularly, met + cela-treated mice exhibited a significant reduction in the IκBκB level (Online Resource 12, panel a). Moreover, a significant reduction in the level of IκBα was observed in DEN-treated mice compared to Normal group mice, indicating a high level of proteasomal degradation, while this decline was offset in the treatment groups, particularly the combination therapy group (Online Resource 12, panel b). In contrast, a significant increase in the level of NFκB p65 (pSer536) occurred in DEN-treated mice compared to Normal group mice, indicating a high level of NFκB activation, but this enhancement was decreased in the treatment groups, particularly the combination therapy group (Online Resource 12, panel c). Taken together, these data show a high level of NFκB signalling inactivation that is enhanced when cela is combined with met.

Effect on the gene expression levels of TNFR and TLR4

The priming step that activates the NLRP3 inflammasome is NFκB signalling, which is induced through activation of TLR4 or TNFR, resulting in increased expression of NLRP3, pro-IL-1β, and pro-IL-18. We found that met, cela, and, particularly, the combination repressed the DEN-induced elevation in TNFR (Fig. 4a) and TLR4 mRNA expression (Fig. 4b).

Effect on TNF-α and IL-6

HCC is commonly associated with inflammation, and increased levels of the proinflammatory cytokines TNF-α and IL-6 are commonly associated with high tumour incidence and promotion of HCC development. In this context, met, cela and, more prominently, the combination therapy significantly reduced inflammation by decreasing the DEN-induced elevations in the levels of TNF-α (Online Resource 13, panel a) and IL-6 (Online Resource 13, panel b) and curbing the interaction of these cytokines with the inflammasome.

Effect on MMP-2, MMP-9 and VEGF

MMP-2 and MMP-9 are suggested to facilitate aspects of tumour progression, including invasion, metastasis, growth and angiogenesis. Met, cela and, more noticeably, met + cela exhibited a significant decrease in the elevated MMP-2 and MMP-9 levels in the DEN-treated group (Online Resource 14, panel a, b, respectively). Correspondingly, the level of the angiogenesis marker VEGF level was decreased in the same manner (Online Resource 14, panel c).

Effect on the gene expression level of cyclin D1

Cyclin D1 activity is required for the G1/S transition in the cell cycle to induce migration, proliferation and angiogenesis. Met, cela and, more noticeably, met + cela exhibited anti-proliferative activity by significantly decreasing the DEN-induced elevation in the level of cyclin D1 (Online Resource 15).

Effect on the mortality fraction

As shown in Online Resource 16, Kaplan–Meier survival analysis revealed that DEN-treated model mice had higher mortality rates than mice in the other groups.

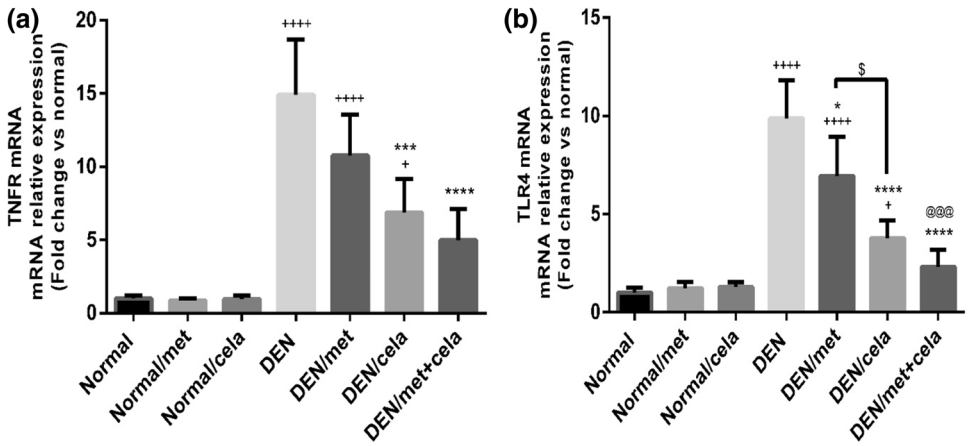

Fig. 4 Effects of met (200 mg/kg), cela (2 mg/kg) and combination therapy on the mRNA relative expression of **a** TNFR, and **b** TLR4 in DEN-induced HCC mouse model. The data are presented as the mean ± SD. $+P < 0.05$ vs. Normal, $++++P < 0.0001$ vs. Normal; $*P < 0.05$ vs. DEN, $***P < 0.001$ vs. DEN, $****P < 0.0001$ vs. DEN; $@@@P < 0.001$ vs. DEN + met

Administration of cela or met + cela decreased the mortality fraction [$p = 0.07$ vs. DEN (Online Resource 16, panel b) and $p = 0.01$ vs. DEN (Online Resource 16, panel c), respectively]. Obviously, consistent with our histological and biochemical analysis results, met chemosensitized HCC model mice to the effect of cela, resulting in enhanced survival benefit.

Discussion

Inflammation is recognized as a predominant cause of the initiation and progression of cancer, including HCC, and the protein expression of NLRP3 is regulated by many factors, including the NFκB pathway [16]. NFκB is a crucial transcriptional regulator of various genes involved in the inflammatory and anti-apoptotic processes of HCC progression. Targeting NFκB has been carefully considered as an appealing approach for the treatment of cancer and has attracted the attention of many researchers in several cancer studies [17].

Accumulating evidence has linked the activation of the NLRP3 inflammasome to HCC [2]. Oligomerization of the inactive inflammasome complex (NLRP3, ASC and caspase-1) regulates the upregulation and maturation of the inflammatory cytokines IL-18 and IL-1β [18]. IL-1β has been established to be involved in the pathogenesis of various cancers [19]. Additionally, inhibitors of the IL-1β and IL-18 cytokines have been studied as a suggested treatment approach for the treatment of breast cancer and osteosarcoma [20]. The process of pyroptosis, a proinflammatory form of programmed cell death mainly mediated by caspase-1, has been reported to be involved in different types of malignancies [21], and in addition to its role in regulating the inflammatory response, the NLRP3 inflammasome has an important role in pyroptosis [22]. The inflammasome activates and cleaves pro-caspase-1 to generate active caspase-1, promoting cell membrane disruption and cell death.

Cela has been established to exert a potent anti-inflammatory effect and strong cytotoxic activity that suppresses tumours in diverse tumour models. Additionally, cela has been widely used to study the antitumour mechanisms in various cancers [23]. Met has been found to inhibit liver cancer cell proliferation both in vitro and in vivo [24]. Several studies have ascribed the antitumour activities of both cela and met to their ability to inhibit NFκB activation [11]. The current research aimed to develop a novel multi-targeted approach by studying the effect of cela and met as combination therapy in the management of HCC. This goal was accomplished by targeting NLRP3 inflammasome activation and its prerequisite, NFκB signalling.

In the present study, in addition to conferring histological improvements and a reduction in the AFP level, met combined with cela showed a significant decrease in the mortality fraction and the numbers of surface nodules per liver compared to cela as a monotherapeutic agent. The combination therapy showed more pronounced anti-inflammatory, anti-proliferative effects. In addition, met + cela combined therapy displayed a remarkable decrease in angiogenesis and metastasis process markers and liver function improvement than either monotherapy. Moreover, the combination therapy showed a marked ability for apoptosis induction and pyroptosis restraint.

Herein, combination therapy with cela and met triggered a marked downregulation of NLRP3 gene expression compared to that in the DEN-treated group. Additionally, diminished caspase-1 activity was seen. Consequently, the IL-1β and IL-18 levels were offset, indicating restraining of pyroptotic activity. In addition, activation of TLR4 and NFκB P65 gene expression are the predominant known stimulators of inflammasome activation. Cela treatment showed a marked downregulation of TLR4 and NFκB P65 gene expression, while coadministration of met increased this effect. These findings shed light on the potential use of met and cela as a valuable therapy in HCC management. Regarding this possibility, our data are consistent with other data demonstrating the effect of cela on the NLRP3 inflammasome pathway [16].

NFκB is both directly and indirectly involved in mediating inflammation, cancer cell proliferation, and metastasis and controls resistance to apoptosis-inducing signals [1, 25, 26]. Normally, latent NFκB activation begins in the cytoplasm, primarily by the stimulation of proinflammatory TNFRs and TLRs. IκBκB is the key enzyme in the classical pathway of NFκB activation, acting by phosphorylating IκBα at serine residues. As a result, the NFκB dimer is retained inactive in the cytoplasm. After phosphorylation, IκB proteins are rapidly ubiquitinated and degraded by the proteasome and facilitate the nuclear translocation of NFκB. In turn, after its nuclear translocation, NFκB activates the transcription of target genes, including proinflammatory regulators (TNF-α, IL-1β and IL-6), matrix metalloproteinases (MMP-2 and -9), cell cycle regulators and pro-proliferative proteins (cyclin D1), anti-apoptotic proteins (BCL-2) and growth factors (VEGF) [4, 27-30].

Consistent with this process, our results revealed that combination therapy with cela and met strongly repressed DEN-induced NFκB activation in mice with HCC by interfering with the phosphorylation of IκBκB at Ser177/181. Furthermore, as a result of proteasomal degradation, liver tissues from DEN-treated mice exhibited a significant decline in the IκBα protein level. This decline was overturned by treatment with either drug. Concurrent with the met- or cela-induced increase in the IκBα protein level, we found a significant decline in IκBα mRNA gene expression. The former data were further confirmed by both the drug-induced significant downregulation of P65 gene expression

and the decreased phosphorylated P65 (pSer536):total P65 ratio. Herein, combined therapy triggered a more intense effect than cela as monotherapy. These findings are consistent with other reports that cela and met are potent inhibitors of NFκB activation [11].

TLR stimulators such as TNF-α or IL-1β are considered potent activators of NFκB signalling. Binding of soluble TNF-α to TNFR induces activation of the canonical NFκB pathway and leads to enhanced expression of IL-1β and IL-6, which, in turn, has been associated with tumour growth and metastasis [31]. Actually, inhibition of TNF signalling strongly suppresses the expression of NFκB-dependent target genes, enhances cancer cell apoptosis, curbs tumour proliferation and reduces the resistance of cancer cells to chemotherapeutic agents [32]. Related to the effects of TNF-α, IL-6 enhances the phosphorylation of IκBκB in cancer cells via PI3K/AKT signalling. Up-regulation of TNF-α and IL-6 expression plays a crucial role in inflammation in several types of malignancies, including hepatocarcinogenesis [31]. Our results revealed that drug treatment, particularly combination therapy, significantly downregulated TNFR gene expression. Consistent with the anti-inflammatory effects of both treatments, we demonstrated weakened oxidative stress, as noticeably shown by the significant decrease in MDA levels compared to those in mice with HCC.

Previously, it has been reported that tumour growth, proliferation, survival and resistance to chemotherapy are strongly related to the suppression of the intrinsic (mitochondrial) or extrinsic pathways of apoptosis [33]. The intrinsic apoptotic pathway involves the disruption of the mitochondrial membrane and the release of cytochrome c (cyt. C) and other apoptotic factors. In this process, caspase-9 activation, which then initiates caspase-3 activation, results in the morphological and biochemical changes associated with apoptosis [34]. Additionally, mitochondrial outer membrane permeabilization is mediated by BCL-2 family members, where the anti-apoptotic BCL-2 subfamily regulates apoptosis by antagonizing the function of the pro-apoptotic Bax protein subfamily [35]. Apoptotic pathways are regulated by different stimuli and factors, including NFκB signalling, which promote tumour survival by induction of the apoptosis inhibitor BCL-2 and inhibition of caspases (caspase-3 and -9) [36]. Many studies have attributed the antitumour effect of cela to its pro-apoptotic potential through upregulation of pro-apoptotic Bax expression and downregulation of the anti-apoptotic protein BCL-2 and, moreover, through increased caspase-3 and -9 activity [37]. Similarly, met has been shown to promote apoptosis and inhibit cancer cell viability [38]. Consistent with these data, our results revealed that treatment with cela, but not met, exerted a significant apoptotic effect, as indicated by the decreased levels of BCL-2 but increased levels of Bax, caspase-3 and caspase-9 compared to those in DEN-treated mice. This effect seems to be due to the inhibition of NFκB signalling. In this respect, cela successfully maintained strong pro-apoptotic potential in combination with met as a dual therapy. Our results revealed apoptosis induction and limited pyroptotic activity. Notably, here, caspase-1 and the inflammasome were not required for caspase-3 activation [39].

In conjunction with their apoptotic effect, cela and met were found to exert a regulatory effect on the cell cycle by downregulating cyclin D1 gene expression. Subsequently, both met and cela repressed cell proliferation. A similar effect was proposed by Gwak et al. [40] and Li et al. [41].

Cancer metastasis and invasion are critically dependent on effective angiogenesis and are strongly related to alterations in the extracellular matrix (ECM). ECM remodelling is greatly regulated by matrix metalloproteinases, mainly MMP-2 and MMP-9 [33]. In addition, MMP gene expression is regulated by NFκB activation through the mitogen-activated protein kinase (MAPK) pathway [42, 43]. Moreover, VEGF expression was confirmed to be induced via NFκB signalling activation [4, 25]. Our results revealed that NFκB inhibition by either cela or met can effectively inhibit tumour angiogenesis, metastasis and invasion markers; VEGF, MMP-2, and MMP-9, respectively, compared to those in HCC mice. In this regard, the combination therapy exhibited the greatest potential.

Treatment with cela, met and the combination effectively restored liver function, as indexed by the significant decreases in serum ALT, AST, ALP and γGT levels. In addition, all treatments significantly decreased the level of the common HCC tumour marker AFP. These findings are consistent with those of previous studies [44, 45]

We conclude that the protective effect of met and cela could be attributed, on the one hand, to their ability to inhibit NLRP3 inflammasome activation, which is more effective than inhibiting effector molecules, and, on the other hand, to the inactivation of NFκB signalling (Fig. 5). As a result, apoptosis induction occurred concurrently with pyroptosis inhibition. Additionally, we concluded that simultaneous administration of met and cela appears to have additive benefits in the treatment of HCC compared to cela as a monotherapeutic agent, leading to prolonged survival and enhanced anti-inflammatory and antioxidant activities. Moreover, met and cela downregulated angiogenesis, metastasis and proliferation markers. Therefore, our data propose a novel multi-targeted approach against HCC that warrants further clinical investigation aimed at minimizing costs and side effects by using lower chronic doses of met and cela.

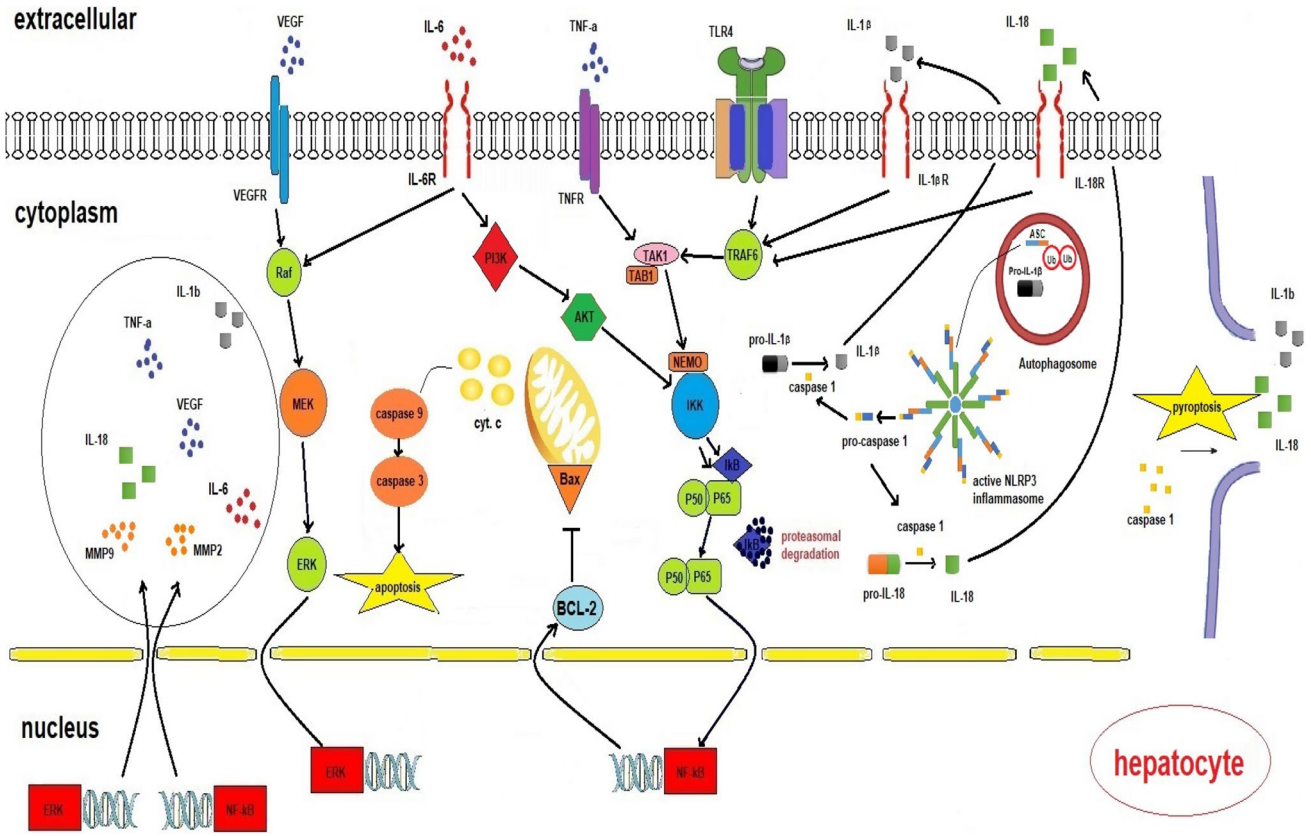

Fig. 5 The proposed mechanism of action

Acknowledgements My deepest sense of gratitude and respectful regards to Dr. Adel Bakeer, professor of pathology, Cairo University, for his indispensable help during the histopathological examination of liver tissues. His long time experience in the field had a remarkable influence on histological interpretations.

Author contributions Conceptualization of this research idea, methodology development, experiments, data collection, data analysis, survival analysis, editing and interpretation were implemented by SS; writing—original draft preparation, interpretation, literature review and analysis were implemented by AMG and EMA; qRT-PCR, ELISA, editing and final revision were implemented by EEA.

Compliance with ethical standards

Conflict of interest The authors have no conflict of interest to declare.

References

1. Saber S, Basuony M, Eldin AS (2019) Telmisartan ameliorates dextran sodium sulfate-induced colitis in rats by modulating NF-κB signalling in the context of PPARγ agonistic activity. Arch Biochem Biophys 671:185–195. https://doi.org/10.1016/j.abb.2019.07.014
2. Fan S-h, Wang Y-y, Lu J, Zheng Y-l, Wu D-m, Li M-q, Hu B, Zhang Z-f, Cheng W, Shan Q (2014) Luteoloside suppresses proliferation and metastasis of hepatocellular carcinoma cells by inhibition of NLRP3 inflammasome. PLoS ONE 9(2):e89961
3. Moossavi M, Parsamanesh N, Bahrami A, Atkin SL, Sahebkar A (2018) Role of the NLRP3 inflammasome in cancer. Molecular cancer 17(1):158
4. Saber S, Mahmoud AAA, Goda R, Helal NS, El-ahwany E, Abdelghany RH (2018) Perindopril, fosinopril and losartan inhibited the progression of diethylnitrosamine-induced hepatocellular carcinoma in mice via the inactivation of nuclear transcription factor kappa-B. Toxicol Lett 295:32–40. https://doi.org/10.1016/j.toxlet.2018.05.036
5. Gilmore TD (2006) Introduction to NF-κB: players, pathways, perspectives. Oncogene 25(51):6680
6. Reghupaty SC, Mendoza R, Sarkar D (2019) AEG-1 targeting for inhibiting inflammation: potential anti-HCC strategy. Oncotarget 10(6):629
7. Zhao Y, Tan Y, Meng T, Liu X, Zhu Y, Hong Y, Yang X, Yuan H, Huang X, Hu F (2018) Simultaneous targeting therapy for lung metastasis and breast tumor by blocking the NF-κB signaling pathway using celastrol-loaded micelles. Drug Deliv 25(1):341–352
8. Konieczny J, Jantas D, Lenda T, Domin H, Czarnecka A, Kuter K, Śmiałowska M, Lasoń W, Lorenc-Koci E (2014) Lack of neuroprotective effect of celastrol under conditions of proteasome inhibition by lactacystin in in vitro and in vivo studies: implications for Parkinson's disease. Neurotox Res 26(3):255–273
9. Yang Q, Yuan H, Chen M, Qu J, Wang H, Yu B, Chen J, Sun S, Tang X, Ren W (2018) Metformin ameliorates the progression

of atherosclerosis via suppressing macrophage infiltration and inflammatory responses in rabbits. Life Sci 198:56–64
10. Niraula S, Dowling RJ, Ennis M, Chang MC, Done SJ, Hood N, Escallon J, Leong WL, McCready DR, Reedijk M (2012) Metformin in early breast cancer: a prospective window of opportunity neoadjuvant study. Breast Cancer Res Treat 135(3):821–830
11. Nguyen TT, Ung TT, Li S, Lian S, Xia Y, Park SY, Do Jung Y (2019) Metformin inhibits lithocholic acid-induced interleukin 8 upregulation in colorectal cancer cells by suppressing ROS production and NF-kB activity. Sci Rep 9 (1):2003.
12. UKCCCR guidelines for the welfare of animals in experimental neoplasia (1988). Br J Cancer 58 (1):109–113. 10.1038/bjc.1988.174
13. Kilkenny C, Browne WJ, Cuthill IC, Emerson M, Altman DG (2010) Improving bioscience research reporting: the ARRIVE guidelines for reporting animal research. PLoS Biol 8(6):e1000412
14. Directive E (2010) 63/EU of the European parliament and of the council of 22 September 2010 on the protection of animals used for scientific purposes. Off J Eur Union 276:33–74
15. Bancroft J, Stevens A, Turner D (1996) Theory and practice of histological techniques 4th Ed Churchill Living Stone, New York Edinburgh. Madrid, Sanfrancisco
16. Xin W, Wang Q, Zhang D, Wang C (2017) A new mechanism of inhibition of IL-1β secretion by celastrol through the NLRP3 inflammasome pathway. Eur J Pharmacol 814:240–247
17. Chen JC-H, Chuang H-Y, Hsu F-T, Chen Y-C, Chien Y-C, Hwang J-J (2016) Sorafenib pretreatment enhances radiotherapy through targeting MEK/ERK/NF-κB pathway in human hepatocellular carcinoma-bearing mouse model. Oncotarget 7(51):85450
18. Hu H, Wang Y, Ding X, He Y, Lu Z, Wu P, Tian L, Yuan H, Liu D, Shi G (2018) Long non-coding RNA XLOC_000647 suppresses progression of pancreatic cancer and decreases epithelial–mesenchymal transition-induced cell invasion by down-regulating NLRP3. Mol Cancer 17(1):18
19. Karki R, Man SM, Kanneganti T-D (2017) Inflammasomes and cancer. Cancer Immunol Res 5(2):94–99
20. Guan Y, Zhang R, Peng Z, Dong D, Wei G, Wang Y (2017) Inhibition of IL-18-mediated myeloid derived suppressor cell accumulation enhances anti-PD1 efficacy against osteosarcoma cancer. J Bone Oncol 9:59–64
21. Cui J, Zhou Z, Yang H, Jiao F, Li N, Gao Y, Wang L, Chen J, Quan M (2019) MST1 suppresses pancreatic cancer progression via ROS-induced pyroptosis. Mol Cancer Res 17(6):1316–1325
22. Wei Q, Zhu R, Zhu J, Zhao R, Li M (2019) E2-induced activation of the NLRP3 inflammasome triggers pyroptosis and inhibits autophagy in HCC cells. Oncol Res Featur Preclin Clin Cancer Ther 27(7):827–834. https://doi.org/10.3727/096504018X15462920753012
23. Jiang Z, Cao Q, Dai G, Wang J, Liu C, Lv L, Pan J (2019) Celastrol inhibits colorectal cancer through TgF-β1/smad signaling. Onco Targets Therapy 12:509
24. Vacante F, Senesi P, Montesano A, Paini S, Luzi L, Terruzzi I (2019) Metformin counteracts HCC progression and metastasis enhancing KLF6/p21 expression and downregulating the IGF axis. Int J Endocrinol 2019:7570146
25. Saber S, Khodir AE, Soliman WE, Salama MM, Abdo WS, Elsaeed B, Nader K, Abdelnasser A, Megahed N, Basuony M, Shawky A, Mahmoud M, Medhat R, Eldin AS (2019) Telmisartan attenuates *N*-nitrosodiethylamine-induced hepatocellular carcinoma in mice by modulating the NF-κB-TAK1-ERK1/2 axis in the context of PPARγ agonistic activity. Naunyn-Schmiedeberg's Arch Pharmacol. https://doi.org/10.1007/s00210-019-01706-2
26. Saber S, Khalil RM, Abdo WS, Nassif D, El-Ahwany E (2019) Olmesartan ameliorates chemically-induced ulcerative colitis in rats via modulating NFκB and Nrf-2/HO-1 signaling crosstalk. Toxicol Appl Pharmacol 364:120–132. https://doi.org/10.1016/j.taap.2018.12.020
27. Saber S, Mahmoud AAA, Helal NS, El-Ahwany E, Abdelghany RH (2018) Renin-angiotensin system inhibition ameliorates CCl4-induced liver fibrosis in mice through the inactivation of nuclear transcription factor kappa B. Can J Physiol Pharmacol. https://doi.org/10.1139/cjpp-2017-0728
28. Saber S, Mahmoud A, Helal N, El-Ahwany E, Abdelghany R (2018) Liver protective effects of renin-angiotensin system inhibition have no survival benefits in hepatocellular carcinoma induced by repetitive administration of diethylnitrosamine in mice. Open Access Maced J Med Sci 6(6):955–960. https://doi.org/10.3889/oamjms.2018.167
29. Saber S (2018) Angiotensin II: a key mediator in the development of liver fibrosis and cancer. Bull Natl Res Centre 42(1):18. https://doi.org/10.1186/s42269-018-0020-7
30. Saber S, Goda R, El-Tanbouly GS, Ezzat D (2018) Lisinopril inhibits nuclear transcription factor kappa B and augments sensitivity to silymarin in experimental liver fibrosis. Int Immunopharmacol 64:340–349. https://doi.org/10.1016/j.intimp.2018.09.021
31. Ray AL, Berggren KL, Restrepo Cruz S, Gan GN, Beswick EJ (2018) Inhibition of MK2 suppresses IL-1β, IL-6, and TNF-α-dependent colorectal cancer growth. Int J Cancer 142(8):1702–1711. https://doi.org/10.1002/ijc.31191
32. Roy P, Mukherjee T, Chatterjee B, Vijayaragavan B, Banoth B, Basak S (2017) Non-canonical NFκB mutations reinforce pro-survival TNF response in multiple myeloma through an autoregulatory RelB:p50 NFκB pathway. Oncogene 36(10):1417–1429. https://doi.org/10.1038/onc.2016.309
33. Su Z, Yang Z, Xu Y, Chen Y, Yu Q (2015) Apoptosis, autophagy, necroptosis, and cancer metastasis. Mol Cancer 14(1):48. https://doi.org/10.1186/s12943-015-0321-5
34. Kashyap D, Sharma A, Tuli HS, Sak K, Mukherjee T, Bishayee A (2018) Molecular targets of celastrol in cancer: Recent trends and advancements. Crit Rev Oncol/Hematol 128:70–81
35. Kang MH, Reynolds CP (2009) Bcl-2 inhibitors: targeting mitochondrial apoptotic pathways in cancer therapy. Clin Cancer Res 15(4):1126–1132. https://doi.org/10.1158/1078-0432.ccr-08-0144
36. Dolcet X, Llobet D, Pallares J, Matias-Guiu X (2005) NF-kB in development and progression of human cancer. Virchows Arch 446(5):475–482
37. Zhao N, Wang H, Mu C, Wang Q, Cai Z (2018) Celastrol inhibits growth and increases apoptosis of human lung cancer A549 cells. Chin J Cell Mol Immunol (Xi bao yu fen zi mian yi xue za zhi) 34(12):1111–1115
38. Kim JS, Turbov J, Rosales R, Thaete LG, Rodriguez GC (2019) Combination simvastatin and metformin synergistically inhibits endometrial cancer cell growth. Gynecol Oncol 154(2):432–440. https://doi.org/10.1016/j.ygyno.2019.05.022
39. Lamkanfi M, Kanneganti T-D, Van Damme P, Berghe TV, Vanoverberghe I, Vandekerckhove J, Vandenabeele P, Gevaert K, Núñez G (2008) Targeted peptidecentric proteomics reveals caspase-7 as a substrate of the caspase-1 inflammasomes. Mol Cell Proteomics 7(12):2350–2363
40. Gwak H, Kim Y, An H, Dhanasekaran DN, Song YS (2017) Metformin induces degradation of cyclin D1 via AMPK/GSK3β axis in ovarian cancer. Mol Carcinog 56(2):349–358. https://doi.org/10.1002/mc.22498
41. Li X, Wang H, Ding J, Nie S, Wang L, Zhang L, Ren S (2019) Celastrol strongly inhibits proliferation, migration and cancer stem cell properties through suppression of Pin1 in ovarian cancer cells. Eur J Pharmacol 842:146–156. https://doi.org/10.1016/j.ejphar.2018.10.043
42. Chiu C-T, Chen J-H, Chou F-P, Lin H-H (2015) Hibiscus sabdariffa leaf extract inhibits human prostate cancer cell invasion

via down-regulation of Akt/NF-kB/MMP-9 pathway. Nutrients 7(7):5065–5087
43. Abdel-Ghany R, Rabia I, El-Ahwany E, Saber S, Gamal R, Nagy F (2015) Blockade of PGE2, PGD2 receptors confers protection against Prepatent schistosomiasis Mansoni in mice. J Egypt Soc Parasitol. https://doi.org/10.12816/0017911
44. Saber S, Mahmoud A, Helal N, El-Ahwany E, Abdelghany R (2017) Losartan, an angiotensin-II type 1 receptor blocker, attenuates CCl4-induced liver fibrosis with a positive impact on survival in mice. World J Pharm Pharm Sci 5(12):121–126
45. Younis NS, Ghanim AMH, Saber S (2019) Mebendazole augments sensitivity to sorafenib by targeting MAPK and BCL-2 signalling in n-nitrosodiethylamine-induced murine hepatocellular carcinoma. Sci Rep 9(1):19095. https://doi.org/10.1038/s41598-019-55666-x